Comparative Study of Adaptive Network-Based Fuzzy Inference System (ANFIS), k-Nearest Neighbors (k-NN) and Fuzzy c-Means (FCM) for Brain Abnormalities Segmentation

Noor Elaiza Abdul Khalid, Shafaf Ibrahim, Mazani Manaf

***Abstract*—**Complexity of medical imagery is found as challenging problem in **s**egmentation. This paper conducts a comparative study of Adaptive Network-Based Fuzzy Inference System (ANFIS), k-Nearest Neighbors (k-NN) and Fuzzy c-Means (FCM) for brain abnormalities segmentation. The characteristics for each brain component of "*membrane*", "*ventricles*", "*light abnormality*" and "*dark abnormality*" is analyzed by extracting the minimum, maximum and mean grey level pixel values. The segmentation performances of each technique is tested to hundred and fifty controlled testing data which designed by cutting various shapes and size of various abnormalities and pasting it onto normal brain tissues. The tissues are divided into three categories of "*low*", "*medium*" and "*high*" based on the grey level pixel value intensities. The segmentation of light abnormalities outperformed the dark abnormalities. It was proven that the ANFIS returns the best segmentation performances in light abnormalities, whereas the k-NN conversely presented well in dark abnormalities segmentation.

***Keywords*—**Adaptive Network-Based Fuzzy Inference System (ANFIS), k-Nearest Neighbors (k-NN), Fuzzy c-Means (FCM), Brain segmentation.

I. INTRODUCTION

VARIETY of diseases occur in the brain tissue area such as brain tumour, stroke, infarction and haemorrhage. Detection of abnormalities in brain tissue area in different medical images is inspired by the necessity of high accuracy as it deals with human life. Thus, several medical imaging modalities had been introduced to defeat this concern such as Magnetic Resonance Imaging (MRI), Computed Tomography (CT) scan, X-ray and Ultrasound. As compared to the other imaging modalities, MRI has a proven capability to provide high quality medical images [1] and has been widely used especially in brain. To date, brain diseases are detected by imaging only after the appearance of neurological or nervous system symptoms. Schmidt *et al*. [2] stated that no early brain diseases detection strategies can diagnoses individuals that are at risk. Nishimura *et al*. [3] claimed that brain diseases are not easily detected by radiologist and neurologist caused by the similar texture of brain abnormalities which leads to the difficulties during the differential diagnosis. Consequently, radiologist and neurologist used an invasive method by injecting some kind of contrast medium such as gadolinium for detecting brain abnormalities [4].

Segmentation of medical imagery remains as a challenging problem due to the complexity of the images [5]. Brain tissue is a particularly complex structure and its segmentation is an important step for studies in temporal change detection of morphology [6]. Success of MRI in the detection of brain pathologies is very encouraging. However, diagnosis and locations of abnormality are made manually by radiologists. It consumes valuable human resources, error sensitive [7] and making it prone to error [8]. Tool is needed to save time as manual segmentation is tedious, less accurate and require long time to complete [9]. Therefore, extensive effort is needed in order to find reliable and accurate algorithms to solve this difficult problem.

The area of visible tumour or areas deemed to contain tumour is called as Gross tumour volume (GTV). Presently, GTV borderlines are manually delineated on the medical images by clinicians [10]. This is a long and painful task [11] and furthermore this method is unreliable and error sensitive [12, 13]. These problems consequently affect the accuracy of the target volume of irradiation. High speed computing machines on the other hand enable the observation of the volume and location of the abnormalities visually [14].

Up till now, there are various segmentation techniques in medical imaging depending on the region of interest [15]. In recent years, medical image segmentation problems has been approached with several solution methods by different range of

Manuscript received August 3, 2011: Revised version received August 3, 2011. This work was supported by the management of Research Management Institute (RMI), UiTM and financial support from E-Science Fund (06-01-01-SF0306) under the Minister of Science, Technology and Innovation (MOSTI), Malaysia.

Shafaf Ibrahim is with the Faculty of Computer and Mathematical Sciences, University Technology MARA, Shah Alam, Selangor, Malaysia, phone: 6019-2692717; fax: 604-5941023 (e-mail: shafaf_ibrahim@yahoo.com).

Noor Elaiza Abdul Khalid is with the Faculty of Computer and Mathematical Sciences, University Technology MARA, Shah Alam, Selangor, Malaysia. (e-mail: elaiza@tmsk.uitm.edu.my).

Mazani Manaf is with the Faculty of Computer and Mathematical Sciences, University Technology MARA, Shah Alam, Selangor, Malaysia (e-mail: mazani@tmsk.uitm.edu.my).

applicability such as Particle Swarm Optimization [16], Genetic Algorithm [17], Adaptive Network-based Fuzzy Inference System (ANFIS) [18], [59], Region Growing [19]-[21], Active Contour Snake model [19], Self Organizing Map (SOM) [22] and Fuzzy c-Means (FCM) [23]. However, segmenting the brain internal structures remains a challenging task due to their small size, partial volume effects, anatomical variability and the lack of clearly defined edges [24]. Thus, considerable effort is required in order to find reliable and accurate algorithms to solve this difficult problem [25]. The most relevant ones for our problem are ANFIS [18], k-NN [32] and FCM [23] segmentation methods. As it showed some potential, the techniques had been tested in brain abnormalities which produced encouraging results.

Fuzzy logics and neural networks are two corresponding technologies. Fuzzy rule-based models are easy to understand because it uses if-then rules structure and linguistic terms. Conversely, the understanding of neural networks knowledge has been difficult since it learns from data and feedback [26]. The hybrid technique of neural networks and fuzzy logic has produced a new technique of neuro-fuzzy system called Adaptive Network-based Fuzzy Inference System (ANFIS) [27]. The implementations of ANFIS in biomedical engineering have been reported to be very effective in various applications such as automatic control, data classification, decision analysis, computer vision [28] as well as medical [29]-[32]. The ANFIS was claimed to be very effective due to its sensitivity and ability of making uncertainty decisions especially in medical applications [30].

K-Nearest Neighbor (k-NN) classification technique is the simplest technique conceptually and computationally that provides good classification accuracy [33]. The k-NN algorithm is based on a distance function and a voting function in k-Nearest Neighbours, the metric employed is the Euclidean distance [34]. The k-NN has higher accuracy and stability for MRI data than other common statistical classifiers, but has a slow running time [35]. Yet, the issues of poor run time performance is not such a problem these days with the computational power that is available [36].

The FCM on the other hand represents a clustering-based method which attempts to classify a voxel to its class using the notion of similarity properties [37]. More specifically, it is a workable soft computing methodology that has been successfully applied in a number of discipline scientific areas such as modelling [38], decision making [39], pattern recognition and classification [40], segmentation [41] as well as medical application areas [42]. In the medical application area, FCM is successfully used to model and analyze the medical process, decision-making [43], [44], image segmentation [39] and tumour grading [45]-[47].

Therefore, this paper conducts a comparative study of the performances of ANFIS, k-NN and FCM techniques by determining the patterns and characteristics for various types of brain tissues. This can be used to segment abnormalities in the human brain in order to identify any existence of brain abnormalities. The basic concept is that the local textures in the images can reveal the characteristic of abnormalities of the biological structures. The accuracy of the segmentation results are then compared with the results obtained by each technique.

The organization of the rest of this paper is as follows: Section II presents our methods, including image mosaicing description, ANFIS, k-NN and FCM algorithms structure. Section III discusses our results and discussions. Finally, we present our conclusion in Section IV.

II. METHODS

The key concept in the segmentation algorithms is the analysis of texture statistics which are used to extract the minimum, maximum and mean value of grey level pixels. It is used as the objective function in all three techniques of ANFIS, k-NN and FCM. It is done by extracting the region of interest (ROI) from the MRI brain images in order to identify the patterns and characteristics of each part in brain tissue area. Subsequently, ANFIS, k-NN and FCM techniques will be applied respectively to segment the abnormality objects from the other brain tissue matters of a MRI brain image.

A. Materials

Hundred and twenty axial slices of Fluid Attenuated Inversion Recovery (FLAIR) sequence brain MRI of normal and abnormal patients are acquired for the testing purposes. The MRI brain images are obtained from adult male and female skulls (age range between 20 to 60 years) from the Department of Diagnostic Imaging, Hospital Kuala Lumpur (HKL).

The prototype of three techniques of ANFIS, k-NN and FCM is developed using Microsoft Borland C++ Builder 6.0. It can be run on a personal computer with a standard WINDOWS platform.

B. Data Analysis

Texture statistics refers to the classification of normal and abnormal brain tissue patterns or texture. Region of interest (ROI) are extracted from the MRI brain images for distinguishing the patterns and characteristics of each part in brain tissue area shown in Fig. 1.

The ROI are divided into four categories of brain component which are:

1) Ventricles
2) Membrane
3) Dark Abnormality
4) Light Abnormality

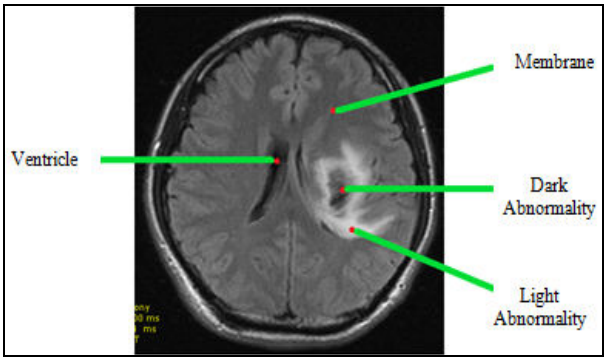

Fig. 1 Proposed areas of brain ROI

Fifty seven ROI data of the four brain component categories had been taken from the MRI images. The ROI image pattern and characteristics are determined by the MinGL, MaxGL and MeanGL as explained in Table I and a summary of the results is shown in Table II.

Table I. Parameters of brain tissue analysis

Parameter	Description
MinGL	Minimum grey level pixel value occurred
MaxGL	Maximum grey level pixel value occurred
MeanGL	Mean of grey level pixel value occurred

Table II. Summary of Reference Table

Brain Component	MinGL	MaxGL	MeanGL
Membrane	69 - 108	99 - 131	86 - 115
Ventricles	7 -55	35 - 92	14 - 66
Dark Abnormality	6 - 53	45 - 118	22 - 83
Light Abnormality	115 - 186	161 - 216	139 – 199

C. *Algorithm and Prototype Construction*

The main process of segmenting abnormalities in a particular MRI brain image is performed during this phase. The techniques of ANFIS, k-NN and FCM are proposed.
Four main stages of the proposed brain abnormalities segmentation algorithm as illustrated in Fig. 2 are:

1) Stage 0: Brain slice selection
   A pre-processing stage in image acquisition works is used to select the brain slices that contain abnormalities. Slices that are free from abnormalities are not processed further.
2) Stage 1: Detection of brain cortical region
   Detects the region of brain cortical using Region growing technique.
3) Stage 2: Removal of brain cortical region
   Removes brain cortical region detected by Stage 1 previously. Regions found to be brain cortical are removed, with those regions remaining labeled as membrane area.
4) Stage 3: Segmentation of abnormalities
   Implements ANFIS, k-NN and FCM techniques for segmentation of abnormalities respectively. Completes the abnormalities segmentation by segmenting the region of abnormalities detected.

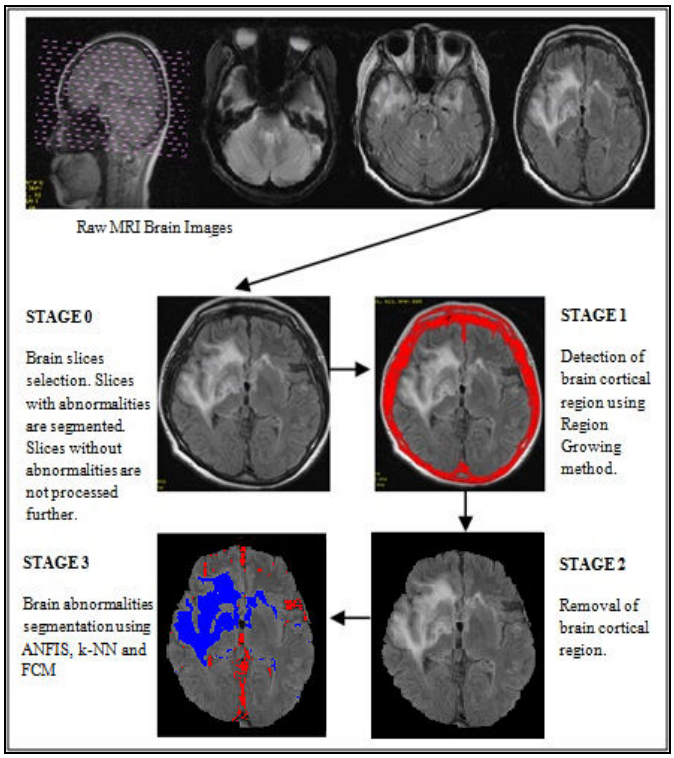

Fig. 2 Proposed brain abnormalities segmentation algorithm

D. *Result Analysis*

The results for this study are evaluated using a method called accuracy check. A total of 120 images, including the 57 images testing images are known to contain abnormalities.

The experiment in this paper uses three types of normal brain tissue intensities background as shown in Table III.

Table III. Background images

Background	Intensity	Min	Max	No of pixels
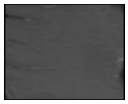	Low	30	114	12144
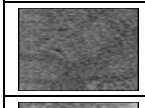	Medium	39	145	12144
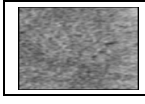	High	56	202	12144

Different shaped ROI of light and dark abnormality are cut and pasted onto the background as tabulated in Table IV. This is used to test out the performance and accuracy of the ANFIS, k-NN and FCM segmentation.

Two methods of analysis are employed to quantify the segmentation accuracy of each technique proposed which are

Receiver Operating Characteristic (ROC) analysis and Pearson's correlation. ROC analysis is a plot of the true positive fraction versus the true negative fraction that produced by classifying each data point as positive and negative according to outcome [48]. It has been effectively used as a statistical validation tools in various areas of segmentation such as mammograms [49], retinal [50], brain [51] and skin [52].

Table IV. Samples of testing images

Background / Abnormality	High	Medium	Low
Light	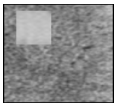	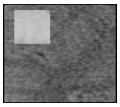	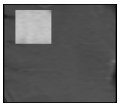
Dark	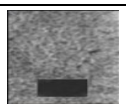	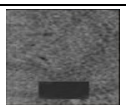	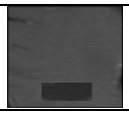

In this paper, the numbers of pixels of the raw MRI brain testing images are compared with the segmented abnormality area. ROC is used to measure the value of false positive, false negative, true positive and true negative. The sample of four conditions areas of false positive, false negative, true positive and true negative during the segmentation are illustrates in Fig. 3.

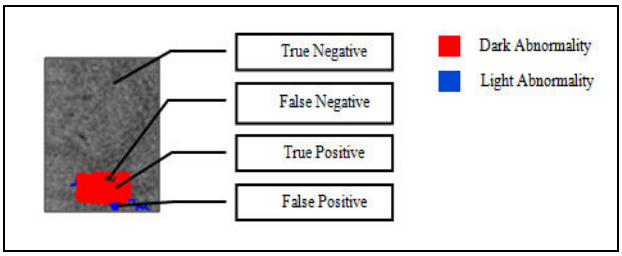

Fig. 3 Sample of testing image of dark abnormality within medium background grey level value after segmentation

The four primary conditions are used to identify the ANFIS, k-NN and FCM segmentation qualities and the level of accuracies for dark and light abnormalities respectively. The descriptions and states for each condition are explained in Table V.

Table V. Primary conditions of accuracy

Condition	Description
False Positive	normal areas that are incorrectly detected as abnormality
False Negative	abnormality areas that are not detected
True Positive	abnormality areas that are correctly detected
True Negative	normal areas that are correctly undetected

The second analysis method employed is Pearson's correlation. Pearson's correlation is widely used to reflect the degree of linear relationship between two variables [53]. In this paper, the Pearson correlation value of three categories between the original abnormalities area versus ANFIS, the original abnormalities area versus k-NN, and the original versus FCM segmentation pixels value are measured using (1) so that the variation of results obtained can be clearly monitored.

$$r = \frac{\sum XY - \frac{\sum X \sum Y}{N}}{\sqrt{\left(\sum X^2 - \frac{(\sum X)^2}{N}\right)\left(\sum Y^2 - \frac{(\sum Y)^2}{N}\right)}} \quad (1)$$

where,

X = number of pixels in original abnormality area
Y = number of pixels in segmented area
N = total number of datasets

E. Adaptive Network-based Fuzzy Inference System (ANFIS)

A detail reviews of the ANFIS model has been given in [54], [55]. A neural-fuzzy system is a hybrid of neural networks and fuzzy systems in such a way that neural networks or neural networks algorithms are used to determine parameters of fuzzy system. The main intention of neural-fuzzy approach is to improve a fuzzy system automatically by means of neural network methods. ANFIS is basically has five layer architectures as shown in Fig. 4.

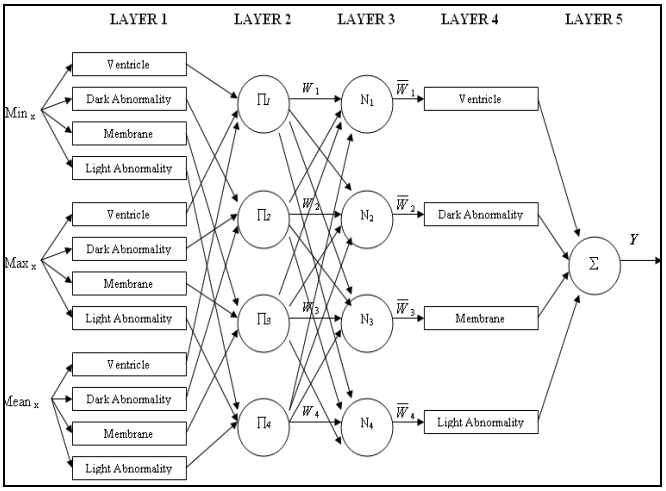

Fig. 4. Proposed ANFIS Architecture

In the first layer, all the nodes are adaptive nodes. The outputs of layer 1 are the fuzzy membership grade of the inputs, which are calculated using (2):

$$o_i^1 = \pi A_i(x) \quad (2)$$

where x is the input to node i and A_i is a linguistic label such as minimum, maximum and mean grey level value associated with the node. O_i^1 is the membership function of A_i and it specifies the degree to which the given x satisfies the

quantifier A_i. $\pi A_i(x)$ is triangle-shaped Membership Function (MF) value ranging from 0 to 1 such as (3):

$$\pi A_i(x) = \frac{1}{1+(x-c_i/a_i)^{2bi}} \quad (3)$$

In the second layer, the nodes are fixed nodes. Each node in this layer represents firing strength of the rules. They are labeled with π, indicating that perform as a simple multiplier. The outputs of this layer can be represented as (4):

$$o_i^2 = w_i = \pi A_i(x_1) \times \pi B_i(x_2) \times \pi C_i(x_3) \ldots \quad (4)$$

where,
I = 1, 2, 3…..n
$x_1, x_2, x_3 \ldots n$ = input
O_i^2 = output of neuron i

In the third layer, the nodes are also fixed nodes labeled by N, to indicate that they play a normalization role to the firing strength from the previous layer. The output of this layer can be represented as (5):

$$o_i^3 = \overline{w}_i = \frac{w_i}{w_1 + w_2 + w_3 + w_4} \quad (5)$$

In the forth layer, the nodes are adaptive. The output of each node in this layer is simply the product of the normalized firing strength and a first order polynomial. Thus, the output of this layer is given by (6):

$$o_i^4 = \overline{w}_i f_i = \overline{w}_i (p_i x_1) + q_i x_2 + r_i x_3 + s_i) \quad (6)$$

Where $\overline{w}_i$ is the output of layer 3 and p_i, q_i and r_i is the parameter set. Parameter in this layer will be referred to as consequent parameters.

In fifth layer, the single layer node is a circle node labeled ∑ that computes the overall output as the summation of all incoming signal as (7):

$$o_i^5 = \sum \overline{w}_i f_i \quad (7)$$

F. K-Nearest Neighbors (k-NN) Algorithm

The second proposed brain abnormalities segmentation technique is based on k-NN paradigm as illustrated in Fig. 5. The k-NN rule is used to construct a lookup table of class, indexed by pixel value.

.

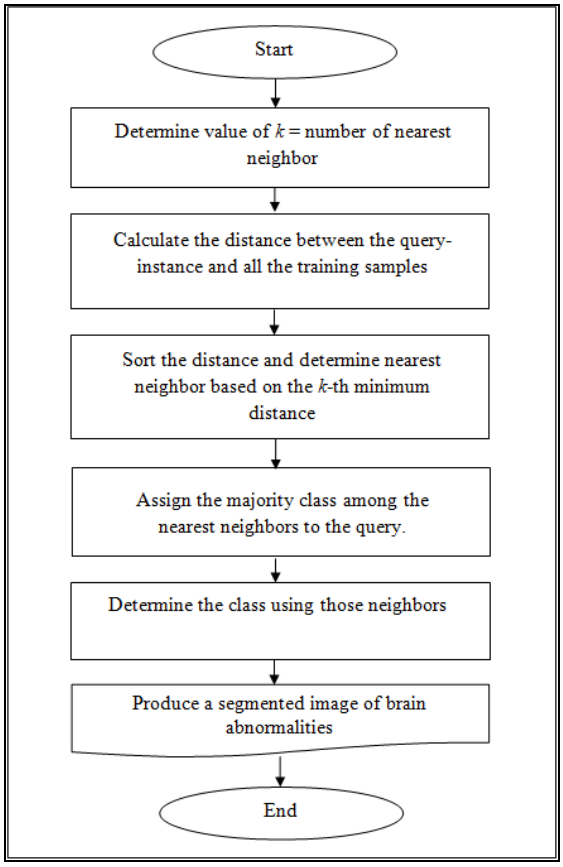

Fig. 5. Proposed steps of k-NN segmentation

The proposed k-NN segmentation is divided into six important steps which are:

Step 1: Determination of *k* value:

k in an important parameter affecting both the accuracy and execution time of the k-NN classification rule is *k*, the number of nearest neighbouring pixels to consider. The choice of variable *k* in k-NN classification is dependent on the relation between the number of features and the number of cases. A small value of *k* may influence the result by individual cases, while a large value of *k* may produce smoother classification outcomes. After a few testing performed, the most suitable value of *k* for this study is *k* = 10.

Step 2: Distance calculation between the query instance and the training samples:

The calculation of distance is executed between the query instance and 150 training samples. The formula of Euclidean distance as in (8) is used as the objective function, which the equation is as follows:

$$d_{ij} = \sum_{k=1}^{n} \left(x_{ik} - x_{jk} \right)^2 \quad (8)$$

where x_{ik} is refers to the instance pixel points, whereas x_{jk} is concerns with the values of training samples. Table VI tabulates a few samples of Euclidean distance calculation

which the value of minimum, maximum and mean grey level values of the query instance is 54, 77 and 79.

Table VI. Samples of Euclidean distance calculations

Min value	Max value	Mean value	Sum of square distance
25	57	36	$[(54-25)^2+(77-57)^2+(79-36)^2]$ = 3090
67	78	69	$[(54-67)^2+(77-78)^2+(79-69)^2]$ = 270
45	73	54	$[(54-45)^2+(77-73)^2+(79-54)^2]$ = 722
14	35	21	$[(54-14)^2+(77-35)^2+(79-21)^2]$ = 6728
34	59	44	$[(54-35)^2+(77-59)^2+(79-44)^2]$ = 1910

Step 3: Sortation of distance based on the k^{th} minimum distance:

After all the Euclidean distances for each query instance are calculated, the distances are then sorted out. As shown in Table VII, the square distances are sorted according to the most minimum square distance produced.

Table VII. Sortation values of square distance

Minimum value	Maximum value	Mean value	Sum of Square Distance	Rank
67	78	69	270	1
45	73	54	722	2
34	59	54	1910	3
25	57	36	3090	4
14	35	44	6728	5

Step 4: Assignment of majority class:

The first 10 (value of *k*) of query instances are then ranked based on the most minimum square distances produced. It will often make sense to assign more weight to the nearest neighbours in deciding the class of the query. Classifying component is based on highest rank [56]. Table VIII shows the result of brain component.

Table VIII. Assignment of majority classes

Brain component	Min value	Max value	Mean value	Sum of Square Distance	Rank
Dark Abnormality	67	78	69	270	1
Dark Abnormality	45	73	54	722	2
Ventricle	34	59	54	1910	3
Membrane	25	57	36	3090	4
Light Abnormality	14	35	44	6728	5

Step 5: Determination of class:

Each query instance is then classified based on the majority categories of brain component it belongs to. From the sample discussed, it can be determined that the query instance is belongs to "ventricles".

Step 6: Segmentation of brain abnormalities:

After each query instance from the overall part of brain image is classified, the brain abnormalities are then identified and segmented.

G. Fuzzy c-Means (FCM) Algorithm

FCM is an iterative algorithm that aims to find cluster centers in an image that minimizes an objective function. A process called as fuzzy partitioning is employed which a data point can belong to all groups with different membership grades between 0 and 1 [57]. The objective function is the sum of squares distance between each pixel and the cluster centers and is weighted by its membership. FCM is defined by six parameters which are shown in Table IX.

Table IX. Parameters for FCM Algorithm

Parameters	Description
n	number of data samples for whole images
c	number of clusters
x_k	k_{th} data sample (Pixel point value)
v_i	i_{th} cluster center
m	weighting exponent (constant greater than unity)
μ_{ki}	membership of x_k in i_{th} cluster

Step 1: Initialize the constants c, m and □ such that:

$1 \le c \le n$

$1 \le m \le \infty$

□ ≥ 0 a small positive constant

Step 2: Initialize the cluster centers:

$$V_0 = (v_{1.0}, v_{2.0} \ldots v_{c.0}) \in R^{CP}$$

For our FCM implementation, the image was clustered into two, which represent abnormality and background based on features values. The algorithm starts by initializing cluster centers to a random value at first time. The performance depends on the initial clusters, thereby allowing running FCM several times, each starting with a different set of initial clusters.

Step 3: Update the membership values, μ_{ki} using (9):

$$u_{ki} = \frac{1}{\sum_{j=1}^{c} \left(\frac{\|x_k - v_i\|}{\|x_k - v_j\|} \right)^{2/(m-1)}} \qquad (9)$$

Different values of may produce different segmentation results. Based on literature, the value of weighting exponent, *m = 2* was used, to get good performance of FCM.

Step 4: Update the cluster centers, v_i using (10):

$$v_i = \frac{\sum_{k=1}^{n} (\mu_{ik})^m x_k}{\sum_{k=1}^{n} (\mu_{ik})^m} \tag{10}$$

Step 5: Check terminating condition, E_t using (11):

$$\text{Let} \quad E_t = \sum_{i=1}^{n} \left\| v_{i,t} - v_{i,t-1} \right\|^2 \tag{11}$$

This process is repeated until the termination condition, E_t is below a certain stopping criteria. Else, repeat step 3 to step 5.

III. Results and Discussion

The numbers of pixels of the raw MRI brain testing images are compared with the ANFIS, k-NN and FCM abnormalities segmented area as illustrated in Table X. Then, every percentage value of false positive, false negative, true positive and true negative are measured by relating the results to any certain circumstances.

Table X. ANFIS vs K-NN vs FCM segmentation

Abnormality	B/Ground	ANFIS	k-NN	FCM
Light	High	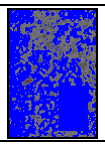	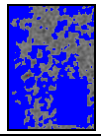	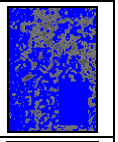
	Medium	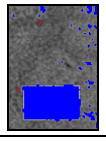	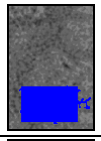	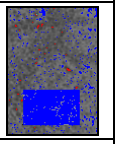
	Low	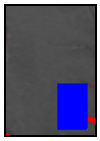	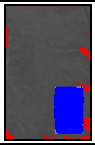	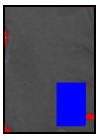
Dark	High	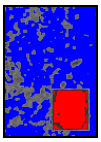	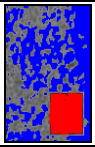	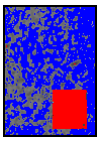
	Medium	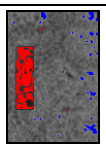	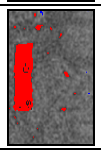	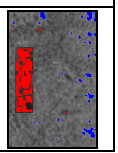
	Low	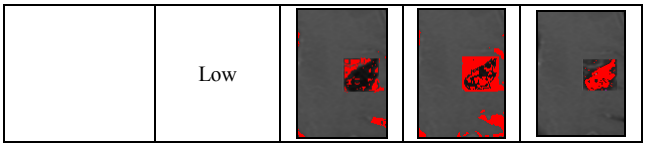		

Table XI tabulates the summary of Receiver Operating Characteristic (ROC) analysis for ANFIS segmentation results. The statistical values obtained are used to quantify the ANFIS segmentation quality and the level of accuracy for dark and light abnormality in three different types of background which are high, medium and low background grey level value.

Table XI. Summary of ROC analysis for ANFIS

Abnormality	B/Ground Grey Level Value	Mean of False Positive	Mean of False Negative	Mean of True Positive	Mean of True Negative
Light	High	0.532	0	1	0.468
	Medium	0.006	0.006	0.994	0.994
	Low	0	0.027	0.973	1
Dark	High	0.578	0.055	0.945	0.422
	Medium	0.004	0.055	0.945	0.996
	Low	0	0.048	0.952	1

The ANFIS is observed to produce an optimum segmentation of light abnormality in medium background intensity as it produced the highest mean values for both true positive and true negative. The performance of light abnormality segmentation in low background intensity also returns good segmentation outcome as it displays excellent mean value of true negative. However, there is slightly lower in the mean of true positive value since it is affected by the small occurrence of false negative. The segmentation of light abnormality within the high background intensity performed unsatisfactorily since it produced the highest mean value of false positive compared to the medium and low background intensity.

For dark abnormality, ANFIS returns the most excellent performance of segmentation in low background intensity since it keeps the mean values for both true positive and true negative at the highest assessment. The combination of dark abnormality within the medium background intensity also cannot be underrated since it produced high mean values for both true positive and true negative. However, small occurrence of false positive and false negative are monitored. The combination of dark abnormality within the high background intensity exhibits poor performance by returning the highest value of false positive.

Conversely, Table XII illustrates the ROC table for k-NN results analysis summary include the same primary conditions as ANFIS too.

Table XII. Summary of ROC analysis for k-NN

Abnormality	Background Gray Level Value	Mean of False Positive	Mean of False Negative	Mean of True Positive	Mean of True Negative
Light	High	0.446	0	1	0.554
	Medium	0.001	0.063	0.937	0.999

	Low	0	0.107	0.893	1
Dark	High	0.004	0.064	0.936	0.996
	Medium	0.023	0.005	0.995	0.977
	Low	0.073	0	1	0.927

From the Table XII, the k-NN is observed to produce almost excellent segmentation performances in medium background grey level value for light abnormality. The statistics show that the combination of light abnormality within the medium background grey level value produced the highest mean values for both true positive and true negative, which are the most important conditions in producing good quality of segmentation. These conditions proved that the k-NN segmentation results showed some potential as the mean values of false positive and false negative are kept at a perfect rate as well. The combination of light abnormality within the low background grey level value is also monitored to produce high mean values for true positive and true negative, although they are slightly less performed than the medium background grey level value. The combination of light abnormality within high background grey level value produced poor segmentation performances since it appears as the highest mean value of false positive compared to medium and low background grey level value. This is found to be caused by the similarity of texture for both light abnormality and high background grey level value that leads the neighbouring pixels to grow outside the abnormality areas.

In contrast, the dark abnormalities segmentation is also successfully performed in medium background grey level value. The combination of dark abnormality within medium background grey level value tend to produce the highest mean values of true positive and true negative as compared to the low and high background grey level values. The combination of dark abnormality within the low background grey level value is also cannot be underestimated as it produced high mean values for both true positive and true negative as well. The result of high background grey level value also produced good segmentation although a small occurrence of false positive mean value is observed.

Conversely, the ROC table for FCM segmentation results analysis summary is tabulated in Table XIII.

Table XIII. Summary of ROC analysis for FCM

Abnormality	B/Ground Grey Level Value	Mean of False Positive	Mean of False Negative	Mean of True Positive	Mean of True Negative
Light	High	0.469	0	1	0.531
	Medium	0.038	0.001	0.999	0.962
	Low	0	0.011	0.989	1
Dark	High	0.413	0.024	0.976	0.587
	Medium	0.003	0.101	0.899	0.997
	Low	0	0.100	0.900	1

As seen from the table above, FCM shows the most excellent segmentation result in low background grey level value for light abnormality. The statistics show that the combination produced the highest mean percentages for both true positive and true negative which are the most important conditions in producing good quality of segmentation. In addition to this, the combination of light abnormality within the medium background grey level value cannot also be underestimated since it produces high mean percentages for both true positive and true negative, although a slight value of mean of false positive can be observed. The combination of light abnormality within the high background grey level value gives a poor performance as it appears to have the highest mean percentage of false positive. This is found to be caused by the texture similarity for both light abnormality and high background grey level value that leads to the neighbouring pixels expanding to grow beyond the abnormality areas.

On the other hand, dark abnormality shows good segmentation result in low background grey level value as it returns the highest mean percentage of true positive and true negative too. However, the mean percentage of false negative shows moderate significance making the process of segmentation of dark abnormality not as good when compares to the segmentation in the light abnormality areas. The mean percentage of false negative appears to increase in the combination of both dark abnormalities within the medium and high background grey level value. This is caused by confusion of the prototype in distinguishing the texture similarity between the dark abnormalities with an anatomical brain structure which is ventricles. Therefore, several improvements for the dark abnormalities segmentation may be necessary to produce better quality of segmentation.

Subsequently, the segmentation performances of ANFIS, k-NN and FCM are compared. The Pearson's correlation value is used to reflect the degree of linearity relationship between the two variables [58]. The correlation value for every original versus ANFIS segmentation pixels value, original versus k-NN segmentation pixels value, and original versus FCM segmentation pixels value are measured as represented in Table XIV.

Table XIV. Pearson's correlation for ANFIS, k-NN and FCM

Abnormality	B/Ground	Original vs ANFIS Correlation	Original vs k-NN Correlation	Original vs FCM Correlation
Light	High	0.89	0.85	0.93
	Medium	0.99	0.99	0.99
	Low	0.99	0.98	0.51
Dark	High	0.62	0.91	0.85
	Medium	0.63	0.88	0.58
	Low	0.62	0.74	0.56

From the table above, it clearly noticed that ANFIS, k-NN and FCM correlation values are almost excellent in light abnormalities segmentation regardless of backgrounds. However, the FCM is monitored to generate considerably low correlation value in low background tissue intensity. For dark abnormalities, the correlation values of the ANFIS and FCM are noted to produce moderate correlation values in all cases. The ANFIS, k-NN and FCM are observed to return the highest correlation values in high background intensity, followed by medium and low background intensities. The overall performances proved that the ANFIS returns the best segmentation performances in light abnormalities, whereas the

k-NN on the other hand performed well in dark abnormalities segmentation.

Table XV tabulates the samples of ANFIS, k-NN and FCM segmentation of MRI brain images for both light and dark abnormalities.

Table XV. Samples of ANFIS, k-NN and FCM Segmentation

Abnormality	MRI Brain Images	ANFIS Segmentation	k-NN Segmentation	FCM Segmentation
Light	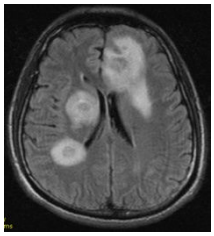	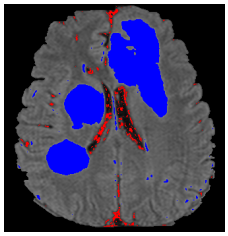	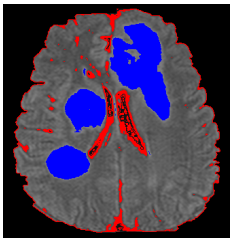	
	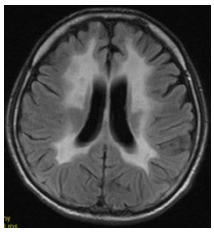	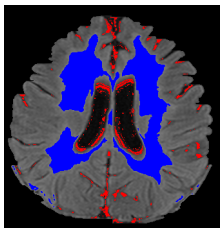	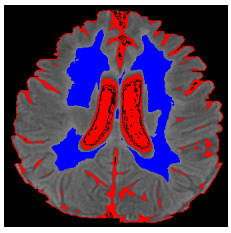	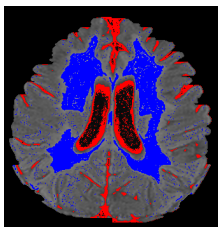
	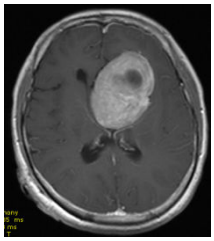	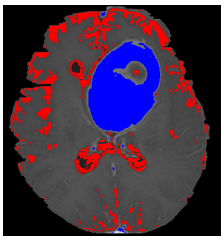	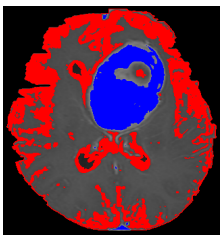	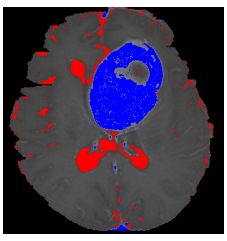
	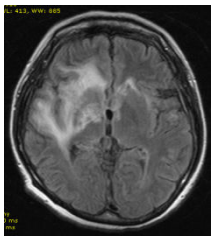	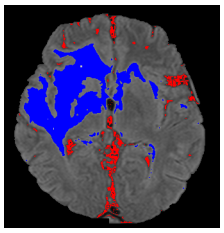	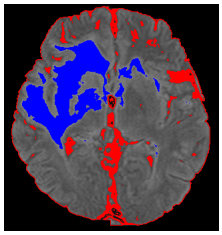	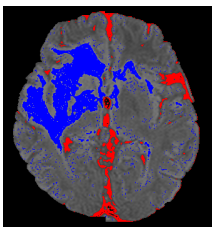
Dark	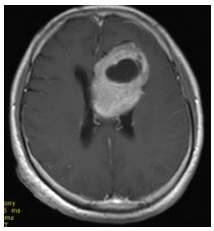	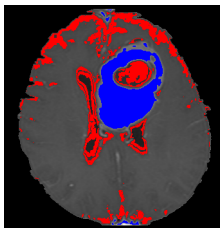	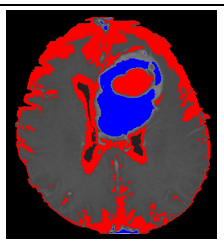	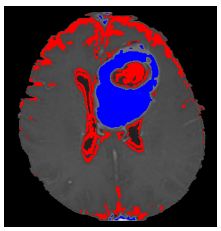
	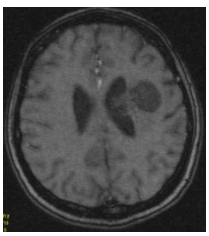	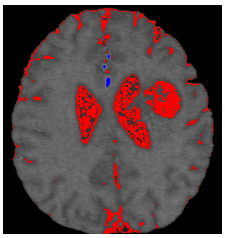	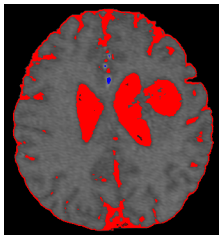	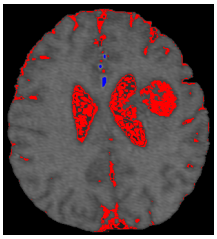

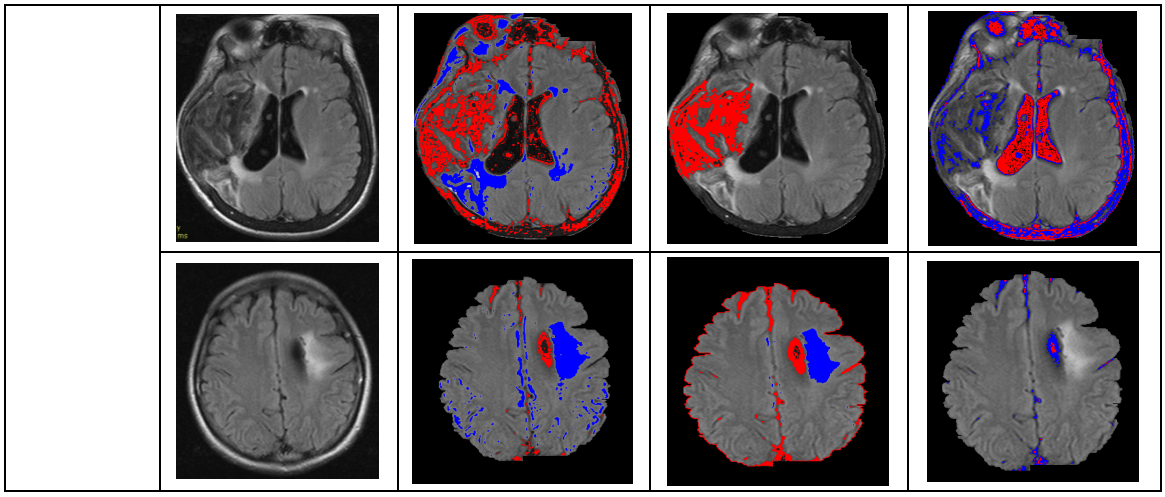

IV. Conclusion

This paper has presented a comparative study of segmentation algorithm performances between three techniques of Adaptive Network-based Fuzzy Inference System (ANFIS), k-Nearest Neighbors (k-NN) and Fuzzy c-Means (FCM) paradigms. All three methods are found to be promising for segmentation of light abnormalities. Nevertheless, the segmentation performances of dark abnormalities are observed to produce moderate significances of correlation values in all conditions. These make the segmentation of dark abnormalities is not as good as segmentation in light abnormalities. It may due to the insensitiveness of the objective function used, setting of parameter values, or deviation of values in data analysis conducted. Several potential improvements are recommended for the future investigation. First, a feature extraction technique could be applied for the recognition of target objects with a homogeneous texture. This is because certain anatomical parts of the brain such as dark abnormality and ventricles could occasionally be confused. The task of integrating the current method of ANFIS, k-NN and FCM with other computer vision architectures could also be proposed in producing better segmentation results in future.

Acknowledgment

The authors acknowledge with gratitude the great support from the management of Research Management Institute (RMI), UiTM and financial support from E-Science Fund (06-01-01-SF0306) under the Minister of Science, Technology and Innovation (MOSTI), Malaysia.

References

[1] Eko Supriyanto, Nurul Afiqah Tahir, Syed Mohd Nooh, "Automatic Ultrasound Kidney's Centroid Detection System", *15th WSEAS International Conference on Computers, Corfu Island, Greece*, July 15-17, pp. 160-165, 2011.

[2] Schmidt M., Levner I., Greiner R., "Segmenting Brain Tumors using Alignment-based Features". *In Proceedings of the Fourth International Conference on Machine Learning and Applications*, 2008.

[3] Nishimura A., Sawada S., Ushiyama I., Tanegashima A., Nakagawa T., Ikemoto K., "Postmortem Diagnosis of Brain Disorders", *Anil Aggrawal's Internet Journal of Forensic Medicine and Toxicology*, Vol. 1, No. 2, 2000.

[4] Singh J., Daftary A., "Iodinated Contrast Media and Their Adverse Reactions", *Journal of Nuclear Medicine Technology*, Vol. 36, No. 2, pp. 69-74, Society of Nuclear Medicine, Teleradiology Solutions, Bangalore, India, 2008.

[5] T. Kapur, "Segmentation of Brain Tissue from Magnetic Resonance Images", Med Image Anal., 1(2): pp. 109-27, June 1996.

[6] Eko Supriyanto, Nor Saradatul Akmar Zulkifli, Mohsen Marvi Baigi, Nasrul Humaimi, Bustanur Rosidi, "Abnormal Tissue Detection of Breast Ultrasound Image using Combination of Morphological Technique", *15th WSEAS International Conference on Computers*, Corfu Island, Greece, July 15-17, pp. 234-239, 2011.

[7] S. Ibrahim, N. E. A. Khalid, and M. Mazani, "Seed-Based Region Growing (SBRG) vs Adaptive Network-Based Inference System (ANFIS) vs Fuzzy c-Means (FCM): Brain Abnormalities Segmentation", International Journal of Electrical and Computer Engineering, WASET, pp. 94-104, Vol. 5, No. 2, 2010.

[8] N. Pradha, and A.K. Sinha, "Development of a composite feature vector for the detection of pathological and healthy tissues in FLAIR MR images of brain", ICGST International Journal on Bioinformatics and Medical Engineering, BIME, Vol. 10, Issue I, pp. 1-11, 2010.

[9] M. A. Masroor, and M. Dzulkifli, "Segmentation of Brain MR Images for Tumour Extraction by Combining Kmeans Clustering and Perona-Malik Anisotropic Diffusion Model", International Journal of Image Processing, 2008, Vol. 2, Issue 1.

[10] Zizzari A., Udo S., Bernd M., Guenther G., Sebastian S., "Detection of Tumour in Digital Images of the Brain", Proceedings of the IASTED International Conference of the Signal Processing, Pattern Recognition and Application, Greece, 2001.

[11] Mancas M., Gosselin B., Macq B., "Segmentation Using a Region-Growing Thresholding", Image Processing: Algorithms and Systems IV, In: Proceedings of the SPIE, Vol. 5672, pp. 388-398, 2005.

[12] Dong-yong D., Condon B., Hadley D., Rampling R., Teasdale G., "Intracranial Deformation Caused by Brain Tumors: Assessment of 3-D Surface by Magnetic Resonance Imaging", *IEEE Transactions on Medical Imaging*, Vol. 12, Issue 4, , pp. 693-702, 1993.

[13] Bouix S., Martin-Fernandez M., Ungar L., Nakamura M., Koo M., McCarley R., Shenton M., "On Evaluating Brain Tissue Classifiers without a Ground Truth", *Neuroimage 07*, 447458, 2007.

[14] Masroor M. A., Dzulkifli M., "Segmentation of Brain MR Images for Tumour Extraction by Combining Kmeans Clustering and Perona-Malik Anisotropic Diffusion Model", *International Journal of Image Processing*, Vol. 2, Issue 1, 2008.

[15] Roerdink J., Meijster A., "The Watershed Transform: Definitions, Algorithms and Parallelization Strategies", Fundamenta Informaticae, pp. 187-228, IOS Press, 2001.

[16] Ibrahim S., Khalid N. E. A., Manaf M., "Empirical Study of Brain Segmentation using Particle Swarm Optimization", *International Conference on Information Retrieval and Knowledge Management*, CAMP'10, 2010.

[17] Ganesan R., Radhakrishnan S., "Segmentation of Computed Tomography Brain Images using Genetic Algorithm*", International Journal of Soft Computing Year 2009*, Vol. 4, Issue 4, pp. 157-161, 2009.

[18] Noor N. M., Khalid N. E. A., Hassan R., Ibrahim S., Yassin I. M., "Adaptive Neuro-Fuzzy Inference System for Brain Abnormality Segmentation", *2010 IEEE Control and System Graduate Research Colloquium*, ICSGRC 2010.

[19] Khalid N. E. A., Ibrahim S., Manaf M., Ngah, U. K., Seed-Based Region Growing Study for Brain Abnormalities Segmentation*, International Symposium on Information Technology 2010* (ITSim 2010), 2010.

[20] Dubey R. B., Hanmandlu M., Gupta S. K., "Semi-automatic Segmentation of MRI Brain Tumor", *ICGST-GVIP Journal*, ISSN: 1687-398X, Vol. 9, Issue 4, August 2009.

[21] Eko Supriyanto, Lai Khin Wee, Yeoh Jing Wui, Nuraini Md Isa, Bustanur Rosidi, "Segmentation of Prostate Tumor For Gamma Image Using Region Growing Method", *15th WSEAS International Conference On Computers*, Corfu Island, Greece, July 15-17, pp.-189-194, 2011.

[22] Iftekharuddin K. M., Zheng J., Islam M. A., Lanningham F., "Brain Tumor Detection in MRI: Technique and Statistical Validation", Fortieth Asilomar Conference on Signals, Systems and Computers, Oct. 29 2006-Nov, pp. 1983-1987, 2006.

[23] Shen S., Snadham W., Granat M., Sterr A., "MRI Fuzzy Segmentation of Brain Tissue using Neighborhood Attraction with Neural Network Optimization", *IEEE Transactions on Information Technology in Biomedicine*, Vol. 9, Issue 3, Sept. 2005, pp. 459-467, 2005.

[24] Linguraru M. G., Ballester M. Á. G., Ayache N., „Deformable Atlases for the Segmentation of Internal Brain Nuclei in Magnetic Resonance Imaging", *International Journal of Computers, Communications & Control,* 2007(II): pp. 26-36.

[25] Chi-Man Pun and Hong-Min Zhu, Textural Image Segmentation Using Discrete Cosine Transform, *3rd International Conference on Communications and Information Technology*, Vouliagmeni, Athens, Greece December 29-31, pp. 54-58, 2009.

[26] Mancas M., Gosselin B., Macq B., "Segmentation using a Region-Growing Thresholding", Proceedings of the SPIE, Image Processing: Algorithms and Systems IV, Vol. 5672, pp. 388-398, 2005.

[27] Yen J., Langari R., "Fuzzy logic: Intelligence", Control and Information. Prentice-Hall Inc., pp. 444, 1999.

[28] Fuzzy Logic Toolbox, "For use with Matlab, user's guide", Version 2, pp. 2–20, The MathWorks, Inc., 2005.

[29] Yu S., Guan L., "A CAD System for the Automatic Detection of Clustered Microcalcification in Digitized Mammogram Films", *IEEE Transactions on Medical Imaging*, 19, pp. 115-126, 2000.

[30] Belal S. Y., Taktak A. F. G., Nevill A. J., Spencer S. A., Roden D., Bevan S., "Automatic Detection of Distorted Plethysmogram Pulses in Neonates and Pediatric Patients using an Adaptive-Network Based Fuzzy Inference System". Artificial Intelligence in Medicine, 24, pp. 149-165, 2002.

[31] Ubeyli E. D., Guler I., "Automatic Detection of Erythematosquamous Diseases using Adaptive Neuro-Fuzzy Inference Systems", Computers in Biology and Medicine, 35, pp. 421-433, 2005.

[32] Ubeyli E. D., Guler I., "Adaptive Neuro-Fuzzy Inference Systems for Analysis of Internal Carotid Arterial Doppler Signals", Comput Biol Med, 2005, in press.

[33] S. Warfield, Duda, "K-Nearest Neighbour Classification", 2001.

[34] A. El-Sayed, El-Dahshan, M. S. Abdel-Badeeh, and H. Y. Tamer, "A Hybrid Technique for Automatic MRI Brain Images Classification", Digital Signal Processing, Vol. 20, Issue 2, March 2010, pp. 433-441.

[35] L. P. Clarke,R. P. Velthuizen, S. Phuphanich, J. D. Schellenberg, J. A. Arrington, and M. Silbiger, "MRI: Stability of Three Supervised Segmentation Techniques", Magnetic Resonance Imaging, 11: pp. 95-106, 1993.

[36] C. P´adraig, and J. D. Sarah, "k-Nearest Neighbour Classifiers", Technical Report UCD-CSI-2007-4, 2007.

[37] Stylios C.D., Groumpos P.P.,"Fuzzy Cognitive Maps in Modeling Supervisory Control Systems" J. Intell. Fuzzy Syst. 8, pp. 83-98, 2000.

[38] Miao Y., Liu Z., "On Causal Inference in Fuzzy Cognitive Maps", IEEE Trans. Fuzzy Syst. 8, pp. 107-119, 2000.

[39] Liu Z., Satur R., "Contextual Fuzzy Cognitive Map for Decision Support In Geographic Information Systems", *IEEE Trans. Fuzzy Syst. 5*, pp. 495-507, 1999.

[40] Chang X., Li W., Farrell J., "A C-means Clustering Based Fuzzy Modeling Method", The Ninth IEEE International Conference on Fuzzy Systems, Vol.2, pp. 937-940, *BIME Journal*, Vol. 06, Issue 1, Dec. 2006.

[41] Kannan S. R., "Segmentation of MRI using New Unsupervised Fuzzy C Mean Algorithm", *ICGST International Journal on Graphics, Vision and Image Processing*, Vol.05, No.2, pp.17-23, January, 2005.

[42] Murugavalli S. Rajamani V., "A High Speed Parallel Fuzzy C-Mean Algorithm for Brain Tumor Segmentation", *BIME Journal*, Volume 6, Issue 1, pp. 29-34, Dec., 2006.

[43] Papageorgiou E.I., Stylios C.D., Groumpos P.P., "An Integrated Two-Level Hierarchical Decision Making System Based on Fuzzy Cognitive Maps*", IEEE Trans. Biomed. Eng.* 50 (12), pp. 1326-1339, 2003.

[44] Liew AWC, Yan H., "An Adaptive Spatial Fuzzy Clustering Algorithm for MR Image Segmentation", *IEEE Trans. Med. Imag.* 2003; 22(9): pp. 1063-75.

[45] Papageorgiou E.I., Spyridonos P. Ravazoula P., Stylios C. D., Groumpos P. P., Nikiforidis G., "Advanced Soft Computing Diagnosis Method for Tumor Grading", Artif. Intell. Med. 36 (1), pp. 59-70, 2006.

[46] Chuang K. S., Tzeng H. L., Chen S., Wu J., Chen T. J,. "Fuzzy c-means clustering with spatial information for image segmentation", Computerized Medical Imaging and Graphics, 30: pp. 9-15, 2006.

[47] Spyridonos P., Papageorgiou E. I., Groumpos P. P., Nikiforidis G., "Integration of Expert Systems with Image Analysis Techniques for Medical Diagnosis", In: Proc ICIAR 2006, Lecture Notes in Computer Science, Vol. 4142, Springer-Verlag, pp. 110-121, 2006.

[48] Gribskov M., Robinson N. L., "Use of Receiver Operating Characteristic (ROC) Analysis to Evaluate Sequence Matching" Comput. Chem., Vol. 20(1), pp. 25-33, 1996.

[49] Qian W., Li L., Clarke L. P., "Image Feature Extraction for Mass Detection In Digital Mammography: Influence of Wavelet Analysis", *The International Journal of Medical Physics Research and Practice*, Vol. 26, Issue 3, 1999.

[50] Joao V. B. S., Jorge J. G. L., Roberto M. C. Jr., Herbert F. J., Michael J. C., "Retinal Vessel Segmentation Using the 2-D Morlet Wavelet and Supervised Classification", *Journal of IEEE Trans Medical Imaging*, Vol. 25, no. 9, pp. 1214-1222, Sep. 2006.

[51] Budde M. D., Kim J. H., Liang H. F., Schmidt R. E., Russell J. H., Cross A. H., Song S. K., "Toward Accurate Diagnosis of White Matter Pathology using Diffusion Tensor Imaging", *Journal of Magnetic Resonance in Medicine*, Vol. 57, Issue 4, pp. 688–695, April 2007.

[52] Sigal L., Sclaroff S., Athitsos V., "Skin Color-Based Video Segmentation under Time-Varying Illumination", *IEEE Transactions on Pattern Analysis and Machine Intelligence*, Vol. 26, Issue 7, pp. 862-877, July 2004.

[53] Trochim W., "*The Research Methods Knowledge Base*", 2nd Edition. Atomic Dog Publishing, 2000, Cincinnati, OH.

[54] Jang J. S. R., Sun C. T., Mizutani E., "Neurofuzzy and soft computing. A Computational Approach to Learning and Machine Intelligent". United States of America. Prentice Hall International, 1997

[55] Nauck D., Klawonn F., Kruse R., "*Foundations of Neuro-Fuzzy Systems*". England. John Wiley & Sons Ltd, 1997.

[56] T. Kardi, "K-Nearest Neighbours Tutorial", available: http:\\people.revoledu.com\kardi\tutorial\KNN.

[57] Albayrak S., Fatih Amasyal F., "Fuzzy c-Means Clustering on Medical Diagnostic Systems", International XII. Turkish Symposium on Artificial Intelligence and Neural Networks (TAINN), 2003.

[58] Shafaf Ibrahim, Noor Elaiza Abdul Khalid, Mazani Manaf, "Evaluation Method for MRI Brain Tissue Abnormalities Segmentation Study", *15th WSEAS International Conference on Computers*, Corfu Island, Greece, July 15-17, pp. 297-302, 2011.

[59] Noor Elaiza Abdul Khalid, Shafaf Ibrahim, Mazani Manaf, "Brain Abnormalities Segmentation Performances Contrasting: Adaptive Network-Based Fuzzy Inference System (ANFIS) vs K-Nearest Neighbors (k-NN) vs Fuzzy c-Means (FCM)", *15th WSEAS International Conference on Computers*, Corfu Island, Greece, July 15-17, pp. 285-290, 2011.

Shafaf Ibrahim is a third semester student of PhD in Science in University Technology MARA, Shah Alam, Malaysia. She holds a Master in Computer Science (2009) and a Bachelor's Degree of Computer Science (2007), all from University Technology MARA. Her research interest covers Image Processing, Medical Imaging, Computer Vision, Artificial Intelligence and Swarm Intelligence.

Dr Noor Elaiza Abdul Khalid is a lecturer in University Technology MARA, Shah Alam, Malaysia. She holds a PhD in Computer Science (2010) from University Technology MARA, a Master in Computer Science (1992) from University of Wales and a Bachelor's Degree of Computer Science (1995) from University Science Malaysia. Her research interests are Swarm Intelligence, Evolutionary Computing algorithms**,** Fuzzy and Medical Imaging.

Assoc. Prof. Dr. Mazani Manaf is a lecturer in University Technology MARA, Shah Alam, Malaysia. He holds respected position at Faculty of Computer Science and Mathematics as Deputy Dean (Student & Alumni), with various professional and community activities and program assessor. His research interest covers Image Processing, Pattern Recognition & Machine Intelligent and Mobile & Distributed Computing.